The 2017 World Congress on
Advances in Structural Engineering and Mechanics (ASEM17)
28 August - 1 September, 2017, Ilsan(Seoul), Korea

Experimental study of cold-formed ferritic stainless steel unlipped channels with web openings subjected to web crippling under interior-two-flange loading

*Amir M. Yousefi[1)] James B.P. Lim[2)] and G. Charles Clifton[3)]

[1), 2), 3)] *Department of Civil and Environmental Engineering, The University of Auckland, New Zealand*
[1)] *ayou561@aucklanduni.ac.nz*

ABSTRACT

Web openings are commonly used in beams of buildings to facilitate services. In this paper, a combination of tests and non-linear finite element analyses is used to investigate the effect of such web openings on the web crippling strength of cold-formed ferritic stainless steel unlipped channel-sections under the interior-two-flange (ITF) loading condition; the cases of both flanges fastened and flanges unfastened to the bearing plates are considered. The results of 54 web crippling tests are presented, with 18 tests conducted on unlipped channel-sections without web openings and 36 tests conducted on sections with circular web openings. In the case of tests with web openings, the circular web openings are located either centred or offset to the bearing plates. A quasi-static finite element model is then presented. Good agreement between the tests and finite element analyses is obtained in terms of failure load, failure modes and post-buckling behaviour.

1. INTRODUCTION

Cold-formed ferritic stainless steels sections are becoming an increasingly attractive choice in buildings due to their combination of price, mechanical properties, and corrosion-resistance (Cashell and Baddoo 2014). The material cost of stainless steel is largely dependent on the nickel content. Compared to austenitic and duplex grades, ferritic grades have no or very low nickel content, and thus have a lower material price.

When used as beams, to provide ease of access for services, the use of web openings are also becoming popular in industry (Lawson *et al.* 2015). Such web openings, however, result in the sections being more susceptible to web crippling, especially under concentrated loads in the vicinity of the openings and also influenced by the position of the openings.

The authors have recently proposed unified strength reduction factor equations for the web crippling strength of cold-formed stainless steel channel-sections with circular web openings under the one-flange loading conditions (Yousefi *et al.* 2016a,b,c, 2017a).

[1)] PhD Scholar
[2)] Associate Professor
[3)] Professor

The equations covered three stainless steel grades: duplex grade EN 1.4462; austenitic grade EN 1.4404 and ferritic grade EN 1.4003. Similar equations for cold-formed carbon steel under end-one-flange loading condition have previously been proposed by Lian *et al.* (2016a,b, 2017a,b), which was a continuation of the work of Uzzaman *et al.* (2012a,b,c, 2013) who had considered the two-flange loading conditions. When applied to the stainless steel grades, (Yousefi *et al.* 2016a,b,c, 2017a) showed that the equations proposed by Lian *et al.* (2016a,b) for the end-one-flange (EOF) loading condition were unconservative by up to 7%. Also, Yousefi *et al.* (2016d, 2017b,c) showed that the equations proposed by Uzzaman *et al.* (2012a, c) for the interior-two-flange (ITF) and end-two-flange loading conditions were unconservative for stainless steel channel-sections. Yousefi *et al. (2017d,e)* also conducted a series of test programme on unlipped cold-formed ferritic stainless steel channels under ITF load and proposed strength reduction factors due to openins in web. The work are summorised in companion study Yousefi *et al. (2017f).*

In the literature, for cold-formed stainless steel lipped channel-sections, only Krovink and van den Berg (1994) and Krovink *et al.* (1995) have considered web crippling strength, but limited to sections without openings. Zhou and Young (2006, 2007, 2008, 2013) have considered the web crippling strength of cold-formed stainless steel tubular sections, again without openings. Research by Lawson *et al.* (2015), while concerned with circular web openings, focussed on the bending strength of the sections and not on the web crippling strength under concentrated loads. In terms of cold-formed carbon steel, Keerthan and Mahendran (2012) considered the web crippling strength of hollow flange channel beams. Sundararajah *et al.* (2016) and Gunalan and Mahendran (2015) have also considered a Direct Strength Method approach for the web crippling strength of channel sections, again without openings. For cold-formed carbon steel lipped channel-sections, recent work has included Natario *et al.* (2014) and Gunalan and Mahendran (2015), all without openings.

In this study, a test programme was conducted on cold-formed ferritic stainless steel unlipped channel sections with circular web openings. The cases of both flanges fastened and flanges unfastened to the bearing plates are considered with the sections subject to interior-two-flange (ITF) loading (see Fig. 1). The finite element modelling presented in this paper uses the general purpose finite element analysis program ABAQUS (2014) for the numerical investigation.

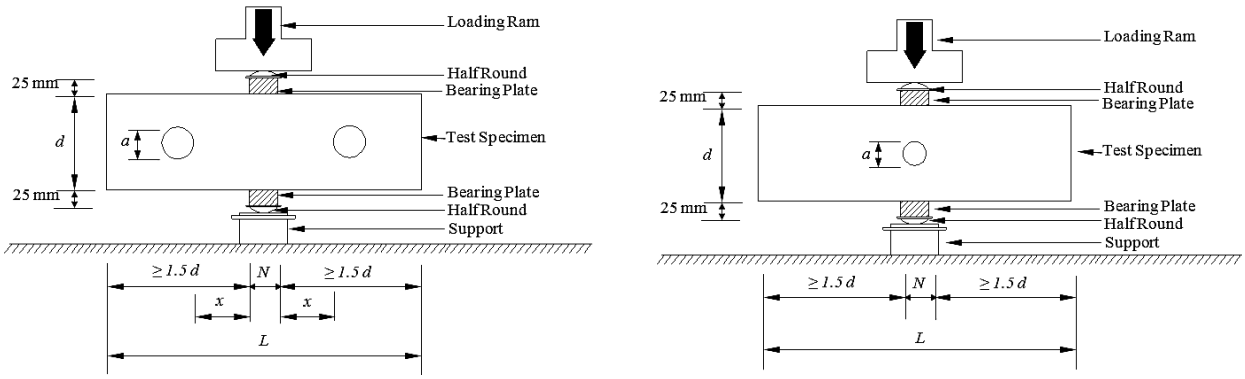

(a) Offset web openings (b) Centred web openings

Fig. 1 Schematic front view of test set-up after Uzzaman et al. (2012a,b)

2. EXPERIMENTAL INVESTIGATION

A test programme was conducted on unlipped channel sections, as shown in Fig. 1, with circular web openings subjected to web crippling. Fig. 2 shows the definition of the symbols used to describe the dimensions of the cold-formed stainless steel unlipped channel sections considered in the test programme. Circular web openings with a nominal diameter (*a*) ranging from 68 mm to 99 mm were considered in the experimental investigation. All test specimens were fabricated with circular web openings located at the mid-depth of the webs and centred to the bearing plates or with a horizontal clear distance to the near edge of the bearing plates (x), as shown in Fig. 1. Channel sections without web openings were also tested. The test specimens consisted three different section sizes; the nominal depth of the webs and the flange widths ranged from 175 mm to 250 mm. The measured web slenderness (*h/t*) values of the channel sections ranged from 154.25 to 251.75. The specimen lengths (*L*) were determined according to the North American Specification (NAS 2016). Generally, the distance between bearing plates was set to be 1.5 times the overall depth of the web (d) rather than 1.5 times the depth of the flat portion of the web (*h*), the latter being the minimum specified in the specification.

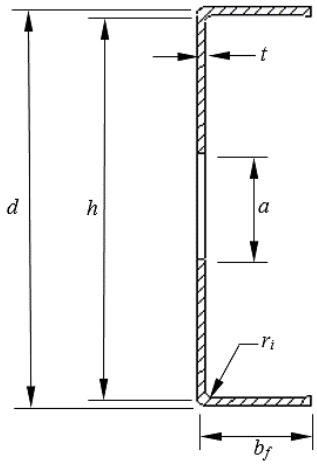

Fig. 2 Definition of symbols


Fig. 3 Tensile coupon test

Tables 1 and 2 show the measured test specimen dimensions for the flanges unfastened and fastened to the bearing plates, respectively, using the nomenclature defined in Figs. 1 and 2 for the ITF loading condition. The bearing plates were fabricated using high strength steel having a nominal yield strength of 550 MPa and a thickness of 25 mm. Three lengths of bearing plates (*N*) were used: 50 mm, 75 mm and 100 mm. In Tables 1 and 2, the specimens were labelled such that the nominal dimension of the specimen and the length of the bearing plates, as well as the ratio of the diameter of the web openings to the depth of the flat portion of the webs (*a/h*) could be identified from the label.

For example, the labels “250x100-t1.2-N75-A0-FR”, “202x100-t1.2-N75-MA0.4-FX” and “202x100-t1.2-N75-OA0.4-FX” are explained as follows:

- The first three notations defined the nominal dimensions (d×b_f–t1.2) of the specimens in millimetres (e.g. 250×75-t1.2 means d = 250 mm; b_f = 100 mm; and t = 1.2 mm).
- ''N75'' indicates the length of bearing in millimetres (i.e. 75 mm).
- '''A0.4'' represents the ratios of the diameter of the circular web openings to the depth of the flat portion of the webs (a/h) i.e. A0.4 means a/h= 0.4.
- “MA0.4” the letter “M” indicates web openings located centred to the bearing plates.
- “OA0.4” the letter “O” indicates web openings located offset to the bearing plates.
- “FR” represents flanges unfastened to the bearing plates and “FX” represents flanges fastened to the bearing plates.

Table 1 Measured specimen dimensions and experimental ultimate loads for flanges unfastened case

Specimen	Web	Flange	Thickness	Filet	Circular web openings		Length	Experimental load per web
	d	b_f	t	r_i	a_{LHS}	a_{RHS}	L	P_{EXP}
	(mm)	(mm)	(mm)	(mm)	(mm)	(mm)	(mm)	(kN)
175x60-t1.2-N50-A0-FR	178.63	60.13	1.13	1.20	-	-	576.00	4.16
175x60-t1.2-N50-MA0.4-FR	178.12	60.27	1.14	1.20	69.00	-	574.83	3.71
175x60-t1.2-N50-OA0.4-FR	178.55	59.98	1.12	1.20	68.89	68.84	574.67	3.29
175x60-t1.2-N75-A0-FR	178.56	60.04	1.12	1.20	-	-	600.67	4.28
175x60-t1.2-N75-MA0.4-FR	178.66	60.05	1.10	1.20	68.74	-	600.17	3.66
175x60-t1.2-N75-OA0.4-FR	178.44	60.09	1.12	1.20	68.80	68.82	600.00	3.34
175x60-t1.2-N100-A0-FR	178.49	60.10	1.12	1.20	-	-	625.67	4.52
175x60-t1.2-N100-MA0.4-FR	178.46	60.11	1.11	1.20	68.87	-	625.00	3.84
175x60-t1.2-N100-OA0.4-FR	178.55	60.09	1.09	1.20	68.70	68.69	625.50	3.41
200x75-t1.2-N50-A0-FR	203.86	74.99	1.09	1.20	-	-	650.00	3.40
200x75-t1.2-N50-MA0.4-FR	203.62	75.01	1.08	1.20	78.92	-	650.33	3.03
200x75-t1.2-N50-OA0.4-FR	203.69	74.92	1.10	1.20	78.69	78.83	650.00	2.85
200x75-t1.2-N75-A0-FR	203.44	75.02	1.08	1.20	-	-	675.67	3.49
200x75-t1.2-N75-MA0.4-FR	203.53	75.06	1.06	1.20	78.90	-	675.67	3.06
200x75-t1.2-N75-OA0.4-FR	203.42	75.11	1.06	1.20	78.93	78.84	675.67	2.77
200x75-t1.2-N100-A0-FR	203.64	74.99	1.12	1.20	-	-	700.33	4.16
200x75-t1.2-N100-MA0.4-FR	203.73	75.02	1.09	1.20	78.93	-	700.67	3.47
200x75-t1.2-N100-OA0.4-FR	203.77	74.84	1.06	1.20	78.90	78.86	700.33	2.86
250x100-t1.2-N50-A0-FR	253.55	100.16	1.02	1.20	-	-	800.67	2.44
250x100-t1.2-N50-MA0.4-FR	253.53	100.78	1.04	1.20	98.81	-	800.33	2.20
250x100-t1.2-N50-OA0.4-FR	253.75	99.73	1.00	1.20	98.87	98.94	801.33	1.91
250x100-t1.2-N75-A0-FR	255.03	100.15	1.07	1.20	-	-	825.67	2.99
250x100-t1.2-N75-MA0.4-FR	254.03	100.24	1.10	1.20	98.82	-	825.67	2.70

250x75-t1.2-N75-OA0.4-FR	253.32	102.47	1.08	1.20	98.86	98.90	825.00	2.51
250x100-t1.2-N100-A0-FR	253.50	99.93	1.11	1.20	-	-	849.50	3.39
250x100-t1.2-N100-MA0.4-FR	253.45	100.04	1.08	1.20	98.86	-	849.67	2.82
250x100-t1.2-N100-OA0.4-FR	253.41	99.91	1.09	1.20	98.84	98.83	850.50	2.59

The tensile coupons were prepared and tested according to ISO 6892-1:2009 (2009) extracting from cold-formed ferritic stainless steel G430 (G) sheet. Five coupons were obtained in the longitudinal direction and five coupons in transverse direction. The coupons were tested in an Instron 4469 tensile testing machine with a capacity of 50 kN by gripping both ends with a pair of flat surface clamps, as shown in Fig. 3.

Table 2 Measured specimen dimensions and experimental ultimate loads for flanges fastened case

Specimen	Web	Flange	Thickness	Filet	Circular web openings		Length	Experimental load per web
	d	b_f	t	r_i	a_{LHS}	a_{RHS}	L	P_{EXP}
	(mm)	(mm)	(mm)	(mm)	(mm)	(mm)	(mm)	(kN)
175x60-t1.2-N50-A0-FX	178.40	60.17	1.13	1.20	-	-	575.00	6.51
175x60-t1.2-N50-MA0.4-FX	178.51	60.08	1.13	1.20	68.86	-	575.50	5.44
175x60-t1.2-N50-OA0.4-FX	178.43	60.02	1.08	1.20	68.89	68.80	575.33	4.92
175x60-t1.2-N75-A0-FX	178.30	60.09	1.14	1.20	-	-	600.00	6.63
175x60-t1.2-N75-MA0.4-FX	178.38	60.09	1.12	1.20	68.70	-	600.67	5.51
175x60-t1.2-N75-OA0.4-FX	178.42	60.00	1.08	1.20	68.90	68.85	600.00	5.05
175x60-t1.2-N100-A0-FX	178.43	59.99	1.14	1.20	-	-	625.67	6.81
175x60-t1.2-N100-MA0.4-FX	178.66	60.03	1.12	1.20	68.84	-	625.33	5.67
175x60-t1.2-N100-OA0.4-FX	178.40	60.15	1.10	1.20	68.74	68.87	625.17	5.23
200x75-t1.2-N50-A0-FX	203.68	75.05	1.13	1.20	-	-	650.00	6.32
200x75-t1.2-N50-MA0.4-FX	203.62	75.13	1.10	1.20	78.95	-	649.67	5.11
200x75-t1.2-N50-OA0.4-FX	203.46	75.14	1.07	1.20	78.82	78.93	650.00	4.67
200x75-t1.2-N75-A0-FX	203.63	75.49	1.14	1.20	-	-	675.67	6.53
200x75-t1.2-N75-MA0.4-FX	203.78	75.04	1.13	1.20	78.92	-	675.67	5.42
200x75-t1.2-N75-OA0.4-FX	203.48	75.12	1.08	1.20	78.82	78.87	676.00	4.91
200x75-t1.2-N100-A0-FX	203.61	75.21	1.14	1.20	-	-	700.33	6.61
200x75-t1.2-N100-MA0.4-FX	203.47	75.04	1.12	1.20	78.90	-	701.67	5.52
200x75-t1.2-N100-OA0.4-FX	203.54	75.37	1.09	1.20	78.91	78.83	700.67	5.10
250x100-t1.2-N50-A0-FX	254.17	99.89	1.14	1.20	-	-	800.00	5.83
250x100-t1.2-N50-MA0.4-FX	253.88	99.99	1.10	1.20	98.90	-	800.83	4.72
250x100-t1.2-N50-OA0.4-FX	253.87	99.94	1.09	1.20	98.92	98.83	801.33	4.41
250x100-t1.2-N75-A0-FX	253.87	99.98	1.14	1.20	-	-	824.33	5.95
250x100-t1.2-N75-MA0.4-FX	253.86	100.05	1.09	1.20	98.88	-	824.67	4.86
250x100-t1.2-N75-OA0.4-FX	253.75	99.86	1.07	1.20	98.89	98.75	825.33	4.36
250x100-t1.2-N100-A0-FX	253.55	99.92	1.14	1.20	-	-	849.67	6.09
250x100-t1.2-N100-MA0.4-FX	253.61	100.00	1.12	1.20	98.83	-	850.67	4.97
250x100-t1.2-N100-OA0.4-FX	253.14	100.02	1.09	1.20	98.84	98.83	850.50	4.64

Instron calibrated extensometer of 50 mm gauge length was used to measure the tensile strain of the coupon specimens.Table 3 summarises the average material properties from the five tests undertaken for each direction which includes the measured static 0.2% proof stress and the static tensile strength based on gauge length of 141 mm. The average measured stress–strain curves of the coupon specimens are presented in Yousefi *et al.* (2017d,e). Comparative hot-rolled steel stress strain curves can be found in Yousefi *et al.* (2014) and Rezvani *et al.* (2015).

Table 3 Material properties obtained from tensile coupon tests

Section	Nominal Thickness (mm)	Base metal thickness (mm)	Gauge width (mm)	Gauge length (mm)	Yield stress $\sigma_{0.2}$ (MPa)	Tensile stress σ_u (MPa)
Longitudinal	1.2	1.18	20	141	276	452
Transverse	1.2	1.17	20	141	291	472
Average	---	---	---	---	284	462

The specimens were tested under the interior-two-flange (ITF) loading condition specified in the North American Specification (NAS 2016), as shown in Fig. 4. Two identical bearing plates of the same width were positioned at the end and at the mid-length of each specimen, respectively. Hinge supports were simulated by two half rounds in the line of action of the force. A 100 kN universal testing machine was used to apply a displacement control compressive load to the test specimens at a rate of 0.05 mm per minute (0.05 mm/min).

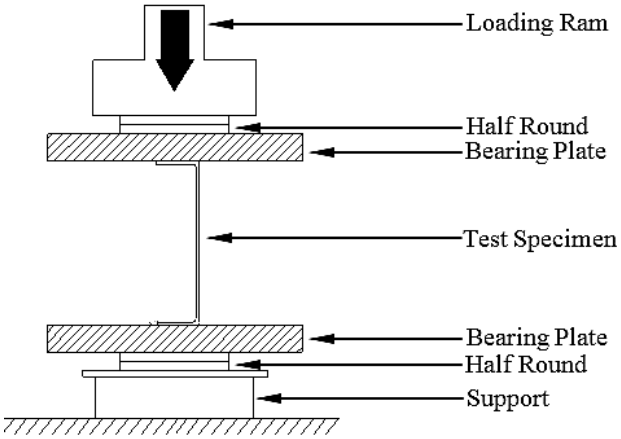

Fig. 4 Schematic end view of test set-up

The load or reaction force was applied by means of bearing plates. All the bearing plates were fabricated using high strength steel having a nominal yield stress of 550 MPa, and thickness of 25 mm. In the experimental investigation, three different lengths of bearing plates (*N*) were used, namely, 50 mm, 75 mm and 100 mm. The experimental investigation also considered flanges of the channel section specimens fastened or unfastened to the bearing plates. For the case of the flanges fastened test set-up, the flanges were bolted to the bearing plates. Photographs of the ITF test is shown in Fig. 5.

A total of 54 specimens were tested under the interior-two-flange (ITF) loading condition. The experimental ultimate web crippling loads per web (P_{EXP}) are given in Tables 1 and 2 for flanges unfastened and fastened cases, respectively. Fig. 6 shows the typical failure mode of web crippling of the specimens with web openings for the flanges fastened to the bearing plates. Typical load-defection curves obtained from the specimen 200×65-t1.2-N50-FX, both without and with web openings are shown in Fig. 7.

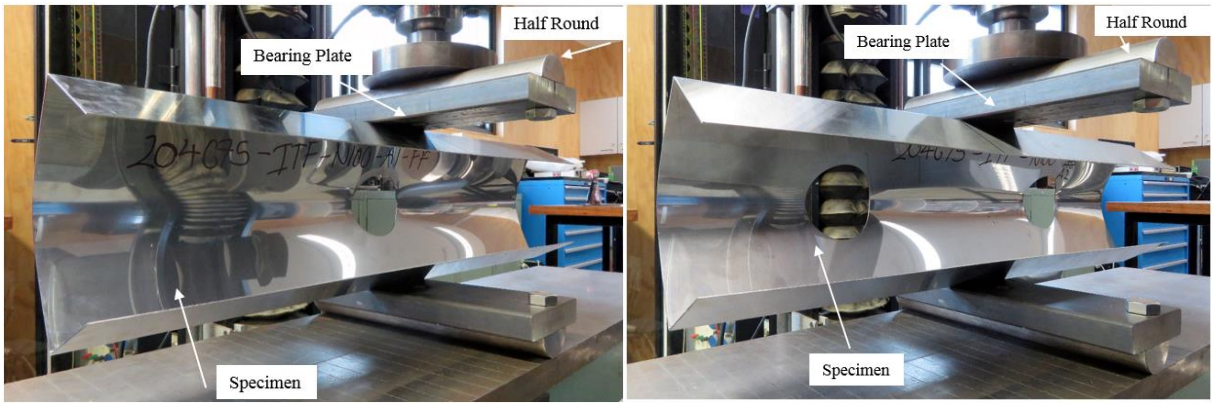

(a) Experimental (b) FEA

Fig. 5 Experimental analysis of cold-formed stainless steel channel sections under ITF loading condition

(a) Offset web openings

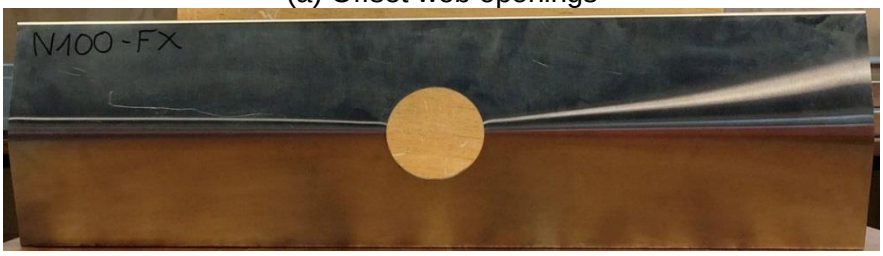

(b) Centred web openings

Fig. 6 Typical failure modes of the specimens

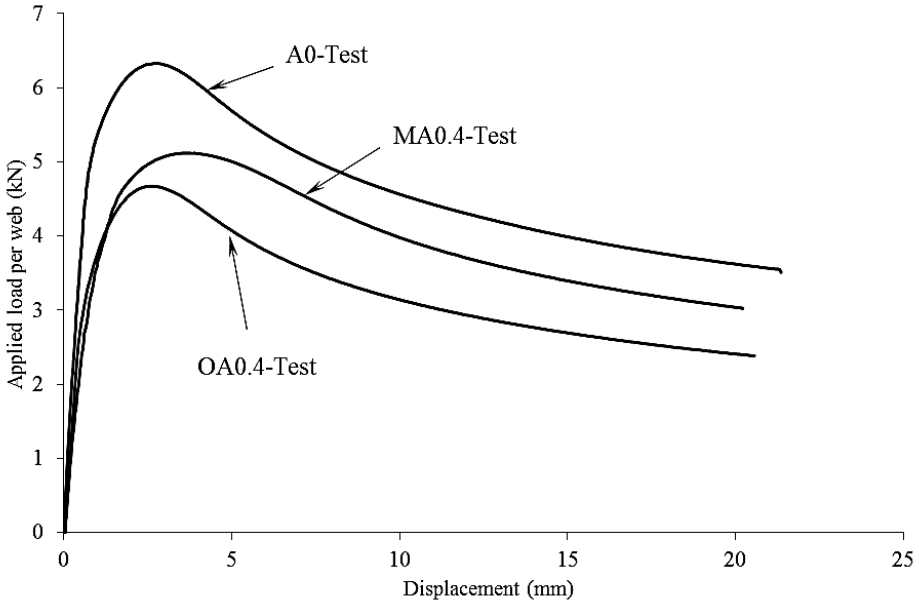

Fig. 7 Web deformation curves for specimen 200×65-t1.2-N50-FX

3. NUMERICAL INVESTIGATION

The finite element (FE) modelling is presented in this paper using the general purpose finite element analysis (FEA) program ABAQUS (2014) for the numerical investigation. In recent studies by the Authors (Yousefi *et al.* 2016d, 2017b), static general analysis was used. In this paper, however, quasi-static analysis was used as it was found that the failure modes and post-buckling behaviour were in better agreement with the laboratory test results; the failure loads were generally unaffected.

Cold-formed stainless steel unlipped channel sections with and without circular web openings were modelled using S4R shell element. The S4R is a four-node double curved thin or thick shell element with reduced integration and finite membrane strains. It is mentioned in the ABAQUS Manual (2014) that the S4R element is suitable for complex buckling behaviour. The S4R has six degrees of freedom per node and provides accurate solutions to most applications. The bearing plates were modelled using analytical rigid plates and C3D8R element, which is suitable for three-dimensional modelling of structures with plasticity, stress stiffening, large deflection, and large strain capabilities. The solid element is defined by eight nodes having three translational degrees of freedom at each node. In the finite element model, the measured cross-section dimensions from the tests were used and the channel sections of the model based on the centreline dimensions of the cross-section were considered.

Fig. 6 shows details of a typical finite element mesh of the channel section and the bearing plates. A mesh sensitivity analysis was used to investigate the effect of different element sizes in the cross-section of the channel sections. Finite element mesh sizes were 5 mm × 5 mm for the cold-formed stainless steel channel sections and 8 mm × 8 mm for the bearing plates.

From the mesh sensitivity analysis, due to the contact between the bearing plates and inside round corners that form the bend between the flanges and web, it was found

that at least five elements were required for the corners between the flanges and web. Finer mesh sizes were used around the web openings when the web openings were modelled.

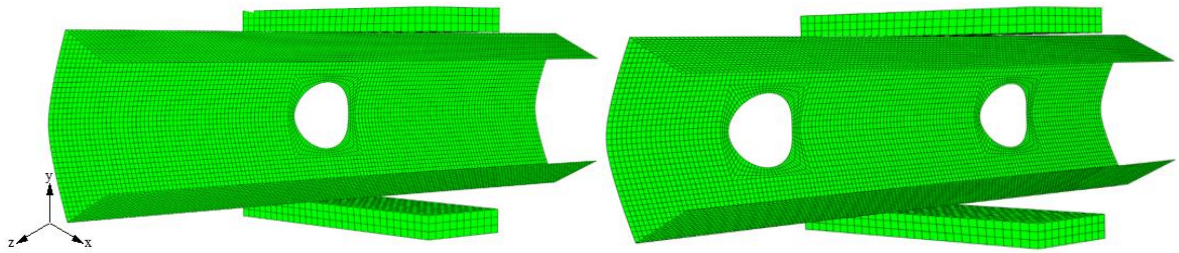

(a) Centred web opening (b) Offset web openings

Fig. 6 Finite element mesh of the specimens

The vertical load applied to the channel section through the bearing plate in the laboratory tests was modelled using displacement control. In the finite element model, a displacement in the vertical y direction was applied to the reference point of the analytical rigid plate that modelled the bearing plate. The top bearing plate was restrained against all degrees of freedom, except for the translational degree of freedom in the Y-direction.

In the shell element idealisation, Cartesian connectors were used to simulate the bolts instead of physically modelling bolts and holes. “CONN3D2” connector elements were used to model the in-plane translational stiffness i.e. x- and z-directions.

The bearing plates, the channel section with circular web openings and the interfaces between the bearing plates and the channel section were modelled. Contact between the bearing plates and the cold-formed stainless steel section was modelled in ABAQUS using the contact pairs option. The bearing plates were the master surfaces, while the cold-formed stainless steel section was the slave surface. The two contact surfaces were not allowed to penetrate each other. A penalty isotropic model with friction equivalent to μ=0.4 was adopted between the surfaces. In the flanges fastened case, in addition to the contact modelled between the bearing plates and the cold-formed stainless steel sections, a connector between the flanges and the bearing plates was modelled at the position of the bolt.

In order to verify and check the accuracy of the finite element model, a comparison between the experimental results and the finite element results were carried out. The comparison of the web crippling strength obtained from the tests (P_{EXP}) and the finite element analysis (P_{FEA}) is shown in Table 4 and Table 5. The comparison of the load-deflection curves for the specimens 200×65-t1.2-N50-FX, without and with web openings, are shown in Fig. 7. It is observed that good agreement has been achieved for both without web openings and with web openings cases.

Table 4 Comparison of web crippling strength predicted from finite element analysis with experiment results for flanges unfastened case

Specimen	Web slenderness	Hole diameter ratio	Exp. load per web	Web crippling strength per web predicted from FEA	Comparison
	(h/t)	(a/h)	P_{EXP}(kN)	P_{FEA}(kN)	P_{EXP}/P_{FEA}
175x60-t1.2-N50-A0-FR	156.08	0.00	4.16	4.16	1.00
175x60-t1.2-N50-MA0.4-FR	154.25	0.39	3.71	3.73	0.99
175x60-t1.2-N50-OA0.4-FR	157.42	0.39	3.29	3.22	1.02
175x60-t1.2-N75-A0-FR	157.43	0.00	4.28	4.31	0.99
175x60-t1.2-N75-MA0.4-FR	160.42	0.39	3.66	3.62	1.01
175x60-t1.2-N75-OA0.4-FR	157.32	0.39	3.34	3.46	0.97
175x60-t1.2-N100-A0-FR	157.37	0.00	4.52	4.49	1.01
175x60-t1.2-N100-MA0.4-FR	158.77	0.39	3.84	3.84	1.00
175x60-t1.2-N100-OA0.4-FR	161.80	0.39	3.41	3.46	0.99
200x75-t1.2-N50-A0-FR	185.03	0.00	3.40	3.52	0.97
200x75-t1.2-N50-MA0.4-FR	186.53	0.39	3.03	3.04	1.00
200x75-t1.2-N50-OA0.4-FR	183.17	0.39	2.85	2.87	0.99
200x75-t1.2-N75-A0-FR	186.37	0.00	3.49	3.65	0.96
200x75-t1.2-N75-MA0.4-FR	190.01	0.39	3.06	3.07	1.00
200x75-t1.2-N75-OA0.4-FR	189.91	0.39	2.77	2.77	1.00
200x75-t1.2-N100-A0-FR	179.82	0.00	4.16	4.35	0.96
200x75-t1.2-N100-MA0.4-FR	184.91	0.39	3.47	3.42	1.01
200x75-t1.2-N100-OA0.4-FR	190.24	0.39	2.86	2.87	1.00
250x75-t1.2-N50-A0-FR	246.58	0.00	2.44	2.51	0.97
250x75-t1.2-N50-MA0.4-FR	241.78	0.39	2.20	2.17	1.01
250x75-t1.2-N50-OA0.4-FR	251.75	0.39	1.91	1.88	1.02
250x75-t1.2-N75-A0-FR	236.35	0.00	2.99	2.94	1.02
250x75-t1.2-N75-MA0.4-FR	228.94	0.39	2.70	2.62	1.03
250x75-t1.2-N75-OA0.4-FR	232.56	0.39	2.51	2.43	1.03
250x100-t1.2-N100-A0-FR	226.38	0.00	3.39	3.39	1.00
250x100-t1.2-N100-MA0.4-FR	232.67	0.39	2.82	2.81	1.00
250x100-t1.2-N100-OA0.4-FR	230.49	0.39	2.59	2.58	1.00
Mean					1.00
COV					0.02

Table 5 Comparison of web crippling strength predicted from finite element analysis with experiment results for flanges fastened case

Specimen	Web slenderness	Hole diameter ratio	Exp. load per web	Web crippling strength per web predicted from FEA	Comparison
	(h/t)	(a/h)	P_{EXP}(kN)	P_{FEA}(kN)	P_{EXP}/P_{FEA}
175x60-t1.2-N50-A0-FX	155.87	0.00	6.51	6.52	1.00
175x60-t1.2-N50-MA0.4-FX	155.98	0.39	5.44	5.44	1.00
175x60-t1.2-N50-OA0.4-FX	163.21	0.39	4.92	4.91	1.00
175x60-t1.2-N75-A0-FX	154.40	0.00	6.63	6.79	0.98
175x60-t1.2-N75-MA0.4-FX	157.27	0.39	5.51	5.50	1.00
175x60-t1.2-N75-OA0.4-FX	163.20	0.39	5.05	5.04	1.00
175x60-t1.2-N100-A0-FX	154.51	0.00	6.81	6.94	0.98
175x60-t1.2-N100-MA0.4-FX	157.52	0.39	5.67	5.64	1.01
175x60-t1.2-N100-OA0.4-FX	160.18	0.39	5.23	5.41	0.97
200x75-t1.2-N50-A0-FX	178.25	0.00	6.32	6.32	1.00
200x75-t1.2-N50-MA0.4-FX	183.11	0.39	5.11	5.15	0.99
200x75-t1.2-N50-OA0.4-FX	188.15	0.39	4.67	4.67	1.00
200x75-t1.2-N75-A0-FX	176.63	0.00	6.53	6.63	0.98
200x75-t1.2-N75-MA0.4-FX	178.34	0.39	5.42	5.59	0.97
200x75-t1.2-N75-OA0.4-FX	186.41	0.39	4.91	4.91	1.00
200x75-t1.2-N100-A0-FX	176.60	0.00	6.61	6.69	0.99
200x75-t1.2-N100-MA0.4-FX	179.67	0.39	5.52	5.60	0.99
200x75-t1.2-N100-OA0.4-FX	184.73	0.39	5.10	5.16	0.99
250x75-t1.2-N50-A0-FX	220.96	0.00	5.83	5.91	0.99
250x75-t1.2-N50-MA0.4-FX	228.80	0.39	4.72	4.78	0.99
250x75-t1.2-N50-OA0.4-FX	230.91	0.39	4.41	4.43	1.00
250x75-t1.2-N75-A0-FX	220.70	0.00	5.95	6.04	0.99
250x75-t1.2-N75-MA0.4-FX	230.90	0.39	4.86	4.88	1.00
250x75-t1.2-N75-OA0.4-FX	235.15	0.39	4.36	4.33	1.01
250x100-t1.2-N100-A0-FX	220.41	0.00	6.09	6.16	0.99
250x100-t1.2-N100-MA0.4-FX	224.43	0.39	4.97	5.00	0.99
250x100-t1.2-N100-OA0.4-FX	230.24	0.39	4.64	4.67	0.99
Mean					0.99
COV					0.01

For the flanges unfastened to the bearing plates, the mean value of the ratio P_{EXP}/P_{FEA} is 1.00 and the corresponding coefficient of variation (COV) was 0.02. A maximum difference of 3% was observed between the experimental and the numerical results for the specimens 250x75-t1.2-N175-MA0.4-FR.

For the flanges fastened to the bearing plates, the mean value of the ratio P_{EXP}/P_{FEA} is 0.99 and the corresponding coefficient of variation (COV) was 0.01. A maximum difference of 3% was observed between the experimental and the numerical results for the specimens 200x75-t1.2-N75-MA0.4-FX.

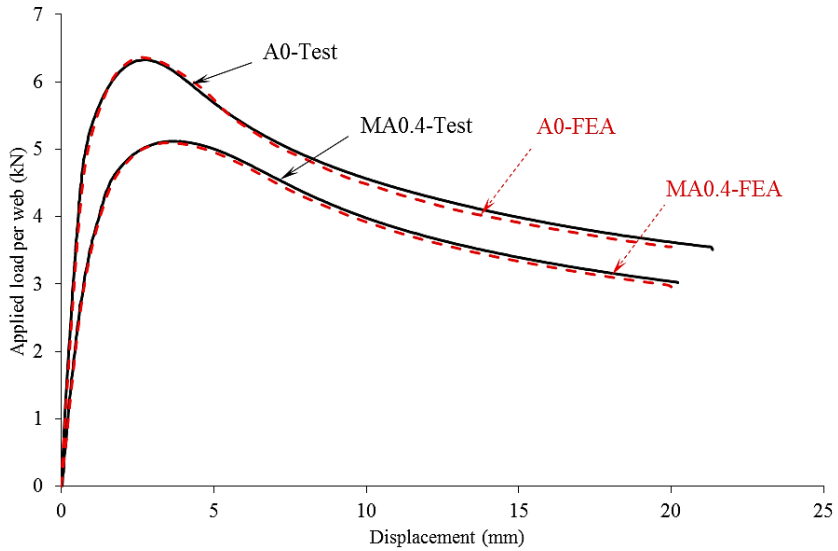

Fig. 7 Comparison of web deformation curves for specimen 200×65-t1.2-N50-FX

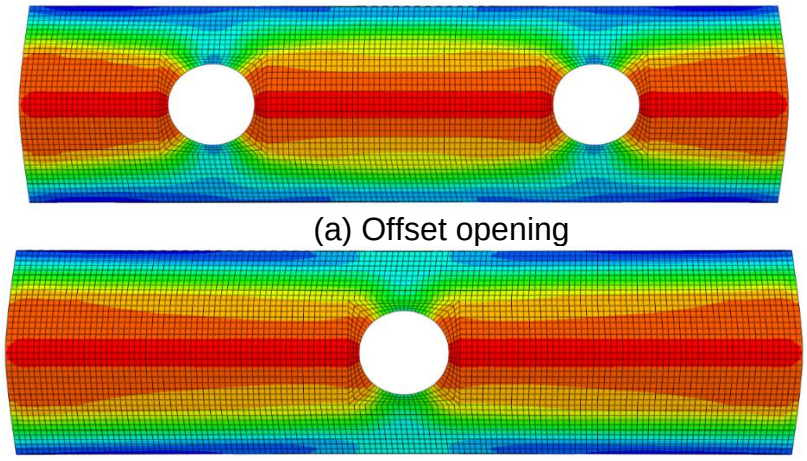

(a) Offset opening

(b) Centred opening

Fig. 8 Typical failure modes of the specimens

The web crippling failure mode observed from the tests has been also verified by the finite element model for the ITF loading condition, as shown in Fig. 8. It is shown that good agreement is achieved between the experimental and finite element results for the web crippling strength, the failure modes and post-buckling behaviour.

4. CONCLUSION

Experimental and numerical investigations on the web crippling behaviour of cold-formed ferritic stainless steel unlipped channel sections, with and without circular web openings, under the interior-two-flange (ITF) loading condition have been presented. A test programme on unlipped channel sections with web openings located at the either centred or offset to the bearing plates were considered. The channel specimens had the measured 0.2% proof stress (yield stress) of 276 MPa and 291 MPa in two sheet

directions. The web slenderness values ranged from 154.25 to 251.75. The ratio of the diameter of the circular web openings to the depth of the flat portion of the webs (*a/h*) was kept constant 0.4 in order to investigate the influence of the web openings on the web crippling behaviour. Flanges of the unlipped channel sections were either fastened or unfastened to the bearing plates.

Quasi-static finite element models were developed and verified against the experimental results in terms of web crippling failure loads, the failure modes and post-buckling behaviour. The finite element models provide a good prediction for web crippling strength of cold-formed ferritic stainless steel unlipped channel sections with and without circular web openings. The verified finite element models can be used to carry out an extended study for developing reliable design recommendations for cold-formed stainless steel unlipped channel sections.

REFERENCES

ABAQUS. (2014), Analysis User's Manual-Version 6.14-2 ABAQUS Inc., USA.

AS/NZS 4600 (2005), Cold-formed steel structures: AS/NZS 4600:2005, Standards Australia, Sydney, Australia.

ASCE 8-02 (2002), Specification for the Design of Cold-Formed Stainless Steel Structural Members: SEI/ASCE 8-02, Reston, VA.

BS 5950-5 (1998), Structural use of steelwork in buildings, Part 5 Code of practice for the design of cold-formed sections. British Standards Institution, London.

Cashell, K. A., and Baddoo, N. R. (2014). "Ferritic stainless steels in structural applications." Thin-Wall. Struct., 83, 169-181.

Gunalan, S., M. Mahendran (2015), "Web crippling tests of cold-formed steel channels under two flange load cases", Journal of Constructional Steel Research, 110, 1-15.

Eurocode-3 (2006), Design of steel structures: Part 1.3: General rules — Supplementary rules for cold-formed thin gauge members and sheeting, in: ENV 1993-1-3, European Committee for Standardization, Brussels, Belgium.

ISO E. 6892-1. (2009). "Metallic Materials: Tensile Testing: Part 1: Method of Test at Room Temperature" ISO E. 6892-1, International Standard, Geneva.

Keerthan, P., and Mahen Mahendran (2012), "Shear behaviour and strength of LiteSteel beams with web openings", Advances in Structural Engineering, 15(2), 171-184.

Korvink, S. A., Van den Berg, G. J., and Van der Merwe, P. (1995). "Web crippling of stainless steel cold-formed beams." J. Constr. Steel Res., 34(2-3), 225-248.

Korvink, S. A., Van den Berg, G. J. (1994). "Web crippling of stainless steel cold-formed beams."Proc., 12th Int. Specialty Conf. on Cold-Formed Steel Structures, University of Missouri-Rolla, St. Louis, 551-569.

Lawson, R. M., Antonio Basta, Assraf Uzzaman (2015), "Design of stainless steel sections with circular openings in shear", Journal of Constructional Steel Research, 112, 228-241.

Lian, Y., Uzzaman, A., Lim, J. B., Abdelal, G., Nash, D., and Young, B. (2017a). "Web crippling behaviour of cold-formed steel channel sections with web holes subjected to Interior-one-flange loading condition-part I: experimental and numerical investigation." Thin-Wall. Struct., 111, 103-112.

Lian, Y., Uzzaman, A., Lim, J. B., Abdelal, G., Nash, D., and Young, B. (2017b). "Web crippling behaviour of cold-formed steel channel sections with web holes subjected to Interior-one-flange loading condition-Part II: Parametric Study and Proposed Design Equations." Thin-Wall. Struct., 114, 92-106.

Lian, Y., Uzzaman, A., Lim, J. B., Abdelal, G., Nash, D., and Young, B. (2016a). "Effect of web holes on web crippling strength of cold-formed steel channel sections under end-one-flange loading condition–Part I: Tests and finite element analysis." Thin-Wall. Struct., 107, 443-452.

Lian, Y., Uzzaman, A., Lim, J. B., Abdelal, G., Nash, D., and Young, B. (2016b). "Effect of web holes on web crippling strength of cold-formed steel channel sections under end-one-flange loading condition-Part II: Parametric study and proposed design equations." Thin-Wall. Struct., 107, 489-501.

NAS (2007), North American Specification for the Design of Cold-Formed Steel Structural Members: American Iron and Steel Institute, AISI S100-2007, AISI Standard.

Natário, P., N. Silvestre, D. Camotim (2014), "Web crippling failure using quasi-static FE models", Thin-Walled Structures, 84, 34-49.

Rezvani, F. H., Yousefi, A. M., and Ronagh, H. R. (2015), "Effect of span length on progressive collapse behaviour of steel moment resisting frames". Structures, 3, 81-89.

Sundararajah, L., Mahendran, M., Keerthan, P. (2016). Experimental Studies of Lipped Channel Beams Subject to Web Crippling under Two-Flange Load Cases. Journal of Structural Engineering, 04016058.

Uzzaman, A., Lim, J. B., Nash, D., Rhodes, J., and Young, B. (2012a). "Web crippling behaviour of cold-formed steel channel sections with offset web holes subjected to interior-two-flange loading." Thin-Wall. Struct., 50, 76-86.

Uzzaman, A., Lim, J. B., Nash, D., Rhodes, J., and Young, B. (2012b). "Cold-formed steel sections with web openings subjected to web crippling under two-flange loading conditions—part I: Tests and finite element analysis." Thin-Wall. Struct., 56, 38-48.

Uzzaman, A., Lim, J. B., Nash, D., Rhodes, J., and Young, B. (2012c). "Cold-formed steel sections with web openings subjected to web crippling under two-flange loading conditions—Part II: Parametric study and proposed design equations." Thin-Wall. Struct., 56, 79-87.

Uzzaman, A., Lim, J. B., Nash, D., Rhodes, J., and Young, B. (2013). "Effect of offset web holes on web crippling strength of cold-formed steel channel sections under end-two-flange loading condition." Thin-Wall. Struct., 65, 34-48.

Yousefi, A. M., Lim, J. B., Uzzaman, A., Lian, Y., Clifton, G. C., and Young, B. (2016a). "Web crippling strength of cold-formed stainless steel lipped channel-sections with web openings subjected to interior-one-flange loading condition." Steel Compos. Struct., Int. J., 21(3), 629-659.

Yousefi, A. M., James B.P. Lim, Asraf Uzzaman, Ying Lian, G. Charles Clifton, Ben Young (2016b), "Web Crippling Strength of Cold-Formed Duplex Stainless Steel Lipped Channel-Sections with Web Openings Subjected to Interior-One-Flange Loading Condition", Proceeding of The Wei-Wen Yu International Specialty Conference on Cold-Formed Steel Structures, Baltimore, Maryland, USA.

Yousefi, A. M., Lim, J. B. P., Uzzaman, A., Lian, Y., Clifton, G. C., Young, B. (2016c). Web crippling design of cold-formed duplex stainless steel lipped channel-sections with web openings under End-One-Flange loading condition, proceeding of The 11th Pacific Structural Steel Conference Shanghai, China.

Yousefi, A. M., Lim, J. B., Uzzaman, A., Lian, Y., Clifton, G. C., and Young, B. (2017a). "Design of cold-formed stainless steel lipped channel sections with web openings subjected to web crippling under end-one-flange loading condition." Adv. Struct. Eng., 10.1177/1369433216670170.

Yousefi, A. M., Lim, J. B. P., Uzzaman, A., Clifton, G. C., Young, B. (2016d). Numerical study of web crippling strength in cold-formed austenitic stainless steel lipped channels with web openings subjected to interior-two-flange loading, proceeding of The 11th Pacific Structural Steel Conference Shanghai, China.

Yousefi, A. M., Uzzaman, A., Lim, J. B., Clifton, G. C., and Young, B. (2017b). "Numerical investigation of web crippling strength in cold-formed stainless steel lipped channels with web openings subjected to interior-two-flange loading condition." Steel Compos. Struct., Int. J., 23(4), 363-383.

Yousefi, A. M., Uzzaman, A., Lim, J. B., Clifton, G. C., and Young, B. (2017c). "Web crippling strength of cold-formed stainless-steel lipped channels with web perforations under end-two-flange loading." Adv. Struct. Eng., 10.1177/1369433217695622.

Yousefi, A. M., Lim, J. B., and Clifton, G. C. (2017d). "Cold-formed ferritic stainless steel unlipped channels with web openings subjected to web crippling under interior-two-flange loading condition–Part I: Tests and finite element model validation." Thin-Wall. Struct., 116, 333-341.

Yousefi, A. M., Lim, J. B., and Clifton, G. C. (2017e). "Cold-formed ferritic stainless steel unlipped channels with web openings subjected to web crippling under interior-two-flange loading condition–Part II: Parametric study and design equations." Thin-Wall. Struct., 116, 342-356.

Yousefi, A. M., Lim, J. B. P., and Clifton, G. C., (2017f). Experimental study of cold-formed ferritic stainless steel unlipped channels with web openings subjected to web crippling under interior-two-flange loading condition, proceeding of The 2017 International Conference on Steel and Composite Structures (ICSCS17), Ilsan (Seoul), Korea.

Yousefi, A. M., Mojtaba Hosseini and Nader Fanaie (2014), Vulnerability Assessment of Progressive Collapse of Steel Moment Resistant Frames. Trends in Applied Sciences Research, 9: 450-460.

Zhao, O., Leroy Gardner, Ben Young, (2016), Buckling of ferritic stainless steel members under combined axial compression and bending, Journal of Constructional Steel Research, Vol. 117, pp. 35-48.

Zhou, F., and Ben Young (2006), "Yield line mechanism analysis on web crippling of cold-formed stainless steel tubular sections under two-flange loading", Engineering Structures, 28(6), 880-892.

Zhou, F., and Ben Young (2007), "Cold-formed high-strength stainless steel tubular sections subjected to web crippling", Journal of structural engineering, 133(3), 368-377.

Zhou, F., and Ben Young (2008), "Web crippling of cold-formed stainless steel tubular sections", Advances in Structural Engineering, 11(6), 679-691.

Zhou, F., and Ben Young (2013), "Web crippling behaviour of cold-formed duplex stainless steel tubular sections at elevated temperatures", Engineering Structures, 57, 51-62.